Research in Astron. Astrophys. **201?** Vol. **X** No. **XX**, 000–000
http://www.raa-journal.org *http://www.iop.org/journals/raa*

***R**esearch in*
***A**stronomy and*
***A**strophysics*

arXiv:1604.04820v2 [astro-ph.GA] 19 Apr 2016

The core dominance parameter and *Fermi* detection of extragalactic radio sources *

Zhenkuo Liu[1], Zhongzu Wu[1], Minfeng Gu[2]

[1] College of Science, Guizhou University, Guiyang 550025, China.; *zzwu08@gmail.com*
[2] Key Laboratory for Research in Galaxies and Cosmology, Shanghai Astronomical Observatory, Chinese Academy of Sciences, 80 Nandan Road, Shanghai 200030, China

Received ; accepted

Abstract In this paper, by cross-correlating an archive sample of 542 extragalactic radio sources with the *Fermi*-LAT Third Source Catalog(3FGL), we have compiled a sample of 80 γ-ray sources and 462 non-*Fermi* sources with available core dominance parameter(R_{CD}), core and extended radio luminosity; all the parameters are directly measured or derived from available data in the literature. We found that R_{CD} have significant correlations with radio core luminosities, γ-ray luminosity and γ-ray flux respectively; the *Fermi* sources have on average higher R_{CD} than non-*Fermi* sources. These results indicate that the *Fermi* sources should be more compact, and beaming effect should play a crucial role for the detection of γ-ray emission. Moreover, our results also show *Fermi* sources have systematically larger radio flux than non-*Fermi* sources at fixed R_{CD}, indicating larger intrinsic radio flux in *Fermi* sources. These results show a strong connection between radio and γ-ray flux for the present sample and indicate that the non-*Fermi* sources is likely due to low beaming effect, and/or the low intrinsic γ-ray flux, support a scenario in the literature: a co-spatial origin of the activity for the radio and γ-ray emission, suggesting that the origin of the seed photons for the high-energy γ-ray emission is within the jet.

Key words: BL Lacertae objects: active-quasars: active-galaxies: general-quasars: general-galaxies: general-gamma-ray: general

1 INTRODUCTION

Blazars are the most extreme active galactic nuclei(AGN) with characteristic properties such as large and variable polarization, apparent superluminal motion, flat or inverted radio spectra, and a broad continuum from radio through γ-rays (e.g., Urry & Padovani 1995). Because of the launch of the *Fermi* satellite, the whole γ-ray sky almost has been scanning once every three hours since July of 2008 by the Large Area Telescope (e.g., Atwood et al. 2009) on board. The third LAT AGN catalog(3LAC)(Ackermann et al. 2015) and *Fermi*-LAT Third Source Catalog(3FGL)(Acero et al. 2015) showed that among all the *Fermi* detected AGNs(FAGNs), nearly all of them are blazars, while it should be noted that there are far larger number of blazars and other type of AGNs that is not detected by *Fermi*.

The differences between FAGNs and non-*Fermi* AGNs(NFAGNs) have been addressed in the literature. Piner et al. (2012) showed that sources detected with *Fermi* have higher apparent speeds than

*

those sources not detected with *Fermi*. Pushkarev & Kovalev (2012) found that the FAGNs have higher brightness temperature and VLBI core flux densities. Linford et al. (2012) showed that the Fermi detected BL Lacs(FBLs) have longer jets and polarized more often. Wu et al. (2014) selected a sample of 100 FBLs and 70 non-*Fermi* BL Lacs(NFBLs) and found that the Doppler factor and intrinsic radio flux is on average larger in FBLs than in NFBLs. Based on a large sample of blazars, Xiong et al. (2015) found that there are significant differences between *Fermi* blazars and non-*Fermi* blazars for black hole mass, jet kinetic power from "cavity" power, and the broad-line luminosity.

By now, Doppler boosting is believed to be one important answer for the question "why are some sources γ-ray loud and others are γ-ray quiet ?"(Lister et al. 2015; Wu et al. 2014; Linford et al. 2011). Doppler factor δ can directly measure the significance of jet beaming effect; a reliable determination of the Doppler factor, δ, is a key step in studying the physical process for the compact emission regions of AGNs (e.g., Wu et al. 2007). However, the Doppler factor calculation is quite difficult and no reliable method for all the sources(e.g., Wu et al. 2007). According to the beaming model of AGN, the emissions are composed of two parts, that is, the boosted core and the isotropic extended ones (e.g., Fan & Zhang 2003). The R_{CD} is calculated by using the ratio of two parts, R_{CD}=F$_C$/F$_E$, where F$_C$ and F$_E$ is the flux of the boosted core and extended structure respectively(e.g., Orr & Browne 1982). On account of the jet emissions are very strong beamed, the R_{CD} should present the orientation of the jet (e.g., Fan & Zhang 2003). To some extent, the R_{CD} is associated with the beaming effect in AGNs (e.g., Fan et al. 2011). Fan et al. (2006) found a significant correlation between the R_{CD} and the Doppler factor δ derived from the lowest γ-ray flux. It will be effective for us to use R_{CD} instead of Doppler factor to understand the relation between beaming and γ-ray detection of our sources in this work.

Although it is believed that beaming is an important parameter for the detection of γ-ray flux, while other parameters are still unclear. Wu et al. (2014) have shown that Doppler factor is an important parameter of γ-ray detection, the non-detection of γ-ray emission in BL Lacs is likely due to low beaming effect, and/or low intrinsic γ-ray flux. The one important aim of this paper is to test that if it is still valid for the γ-ray detection of other types of AGN. This paper is organized as follows: the sample selection is stated in section 2; the results are showed in section 3; the discussion is presented in section 4, and the summary is given in section 5. Throughout the paper we define the spectral index α as f$_\nu \propto \nu^{-\alpha}$ where f_ν is the flux density at frequency ν and a cosmology with $\mathrm{H}_0 = 70\ \mathrm{km\ s^{-1}\ Mpc^{-1}}$, $\Omega_\mathrm{M} = 0.3$, $\Omega_\Lambda = 0.7$. All values of luminosity used in this paper are calculated with our adopted cosmological parameters.

2 THE SAMPLE

Fan & Zhang (2003) present a large sample of 542 extragalactic radio sources(27 BL Lacs, 215 quasars, and 300 galaxies) with R_{CD} at 5 GHz and other parameters. Under the assumption that the core spectral index is α_C = 0.0 and the extended spectral index is α_E = 0.5 and 1.0 respectively, the $R_{CD}$is derived as: R_{CD}=$\frac{L_C}{L_E}$=$\frac{L_C}{L_T-L_C}$(1.4/5)$^{-\alpha_E}$(1+z)$^{-\alpha_E}$, where L_C is the 5 GHz radio core luminosity, L_E is the 5 GHz extended luminosity, and L_T is the 1.4 GHz total luminosity(see Fan & Zhang (2003) for detail).

In this work, we cross-correlate this sample with the 3FGL(Acero et al. 2015), this offers a sample of 80 γ -ray detected AGNs, including 22 BL Lac objects, 11 radio galaxies, 3 seyfert galaxies and 44 Quasars(see Table. 1). In this work, the γ -ray flux and luminosity is from 100 MeV to 300 GeV energy range. The corresponding results are listed in Table 1, of which Col.1 is the source name, Col.2 is identification(BL stands for BL lacertae objects, Q for quasars, G for radio galaxy, S, S1, S2 for Seyfert galaxies), Col.3 is redshift, Col.4 for total luminosity at 1.4 GHz , Col.5 for core luminosity at 5 GHz , Col.6 and Col.7 are R_{CD} corresponding to α_E =0.5, 1.0 respectively, and Col.8 is the γ-ray luminosity. In total, we have a sample of 542 extragalactic sources containing 80 *Fermi* objects(22 BL Lacs, 44 quasars, and 14 galaxies) and 462 non-*Fermi* objects(5 BL Lacs, 171 quasars, and 286 galaxies).

3 THE RESULTS

To study the differences of FAGNs and NFAGNs, we compare various radio properties for two subsamples, including R_{CD}, the core and extended luminosity. The results are shown as follows.

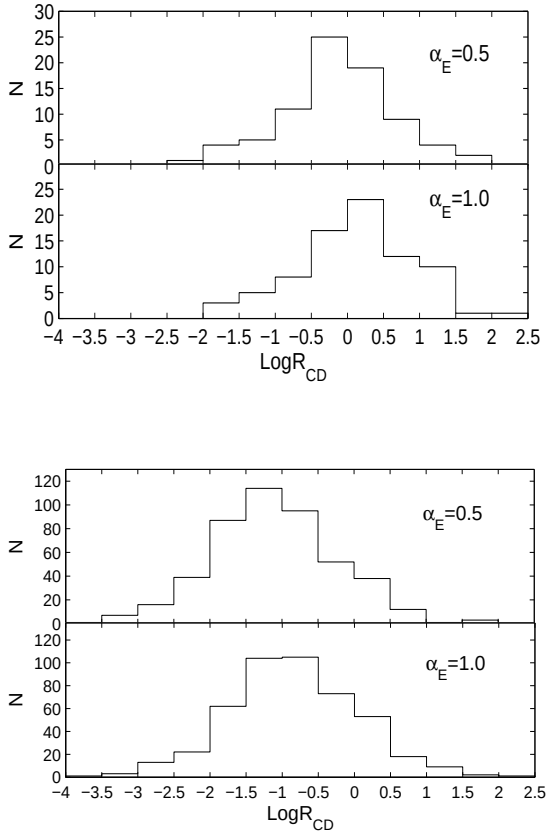

Fig. 1 The logR_{CD} histogram for FAGNs and NFAGNs according to different extended spectral index α_E. The top and bottom panels are the cases for FAGNs and NFAGNs respectively, of which the upper panel is corresponding to α_E=0.5, the bottom panel is α_E=1.0 respectively.

3.1 The distributions of R_{CD} for FAGNs and NFAGNs

Fig.1 shows the R_{CD} distribution of FAGNs and NFAGNs with different extended spectral index, α_E(α_E=0.5 and α_E=1.0 respectively). Through the comparison, we can learn that the distribution of R_{CD} from different extended spectral index α_E is similar for both FAGNs and NFAGNs. Because of their similarity, we adopt only α_E=1.0 for the rest of our results. From Fig.1, we can also find that the R_{CD} of NFAGNs are on average smaller than FAGNs for both of α_E cases. Using non-parametric Kolmogorov-Smirnov(KS) test, we get that the R_{CD} distribution between FAGNs and NFAGNs are significantly different(chance probability P $\sim 10^{-17}$), the mean values for FAGNs and NFAGNs are LogR_{CD}=0.13 and LogR_{CD}=-0.86 respectively.

The R_{CD} distribution of quasars and radio galaxies are shown in Fig.2. Through nonparametric KS test, we find that the R_{CD} distribution between the *Fermi* quasars and non-*Fermi* quasars are significantly different(chance probability $P \sim 10^{-7}$), the mean values are LogR_{CD}=0.40 and LogR_{CD}=-0.43 respectively. While between the *Fermi* galaxies and non-*Fermi* galaxies, the result of KS test shows that there is no significant difference(P=0.713), but the mean value of R_{CD} for the *Fermi*

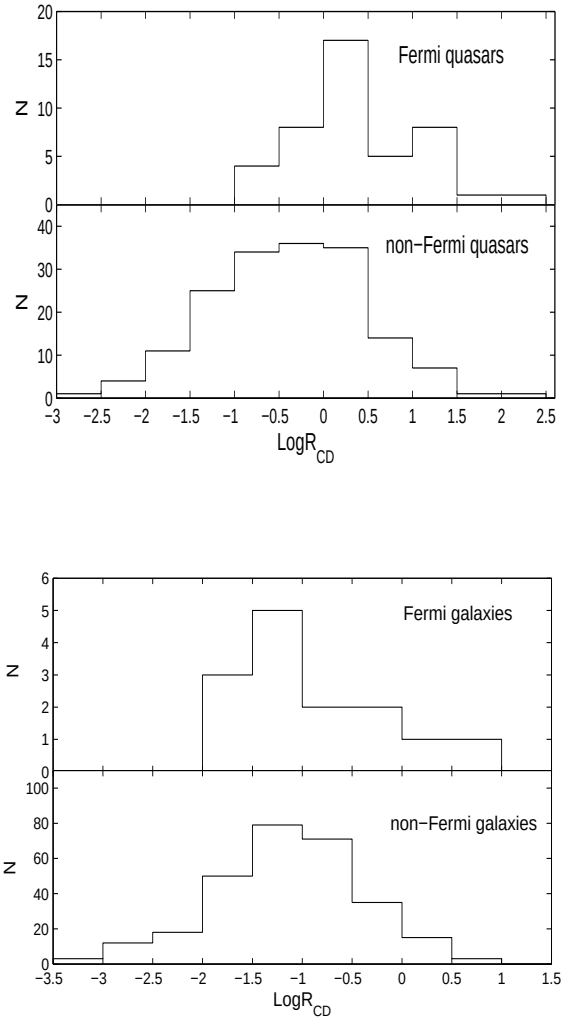

Fig. 2 The histogram comparison of R_{CD} for quasars and galaxies(for each picture the upper panel is *Fermi* sources and bottom panel is non-*Fermi* sources).

galaxies(LogR_{CD}=-0.89) is also higher than the value of non-*Fermi* galaxies(logR_{CD}=-1.14). Because the number of *Fermi* galaxies are very small, which is only 14 in the 300 galaxies, this result might not definite. Additionally, because majority of the BL Lacs(22 of 27) in this sample are detected by *Fermi*, the difference of FBL and NFBLs is not studied in this work, the result of BL Lacs is referred to Wu et al. (2014).

3.2 The radio emission of FAGNs and NFAGNs

In this part, we studied the difference of radio core luminosity for *Fermi* and non-*Fermi* sources and shown in Fig.5. It shows a tendency that the sources detected with *Fermi* have on average higher core-luminosity than sources not detected. From KS test, the distribution of core luminosity between FAGNs and NFAGNs are significant different ($P \sim 10^{-9}$ for all,$P \sim 10^{-5}$ for quasars only). While for galaxies, the result of KS test shows that they do not have significant differences(P=0.458), but the mean values for *Fermi*-galaxies(Log L_c=23.29) is slightly higher than the value of non-*Fermi* galaxies (Log L_c=23.15).

The relations between R_{CD} and logL_C, and between R_{CD} and logL_E are all studied and shown in Fig. 5. We find there are positive correlation between R_{CD} and L_c for both FAGNs and NFAGNs, with correlation coefficient r=0.49 and 0.46 respectively, and all at a confidence level over 99.99% by Spearman rank correlation analysis. According to the beaming model of AGN(Urry & Padovani 1995), the parameters R_{CD} and L_C both rely on Doppler factor δ, R_{CD}= R'_{CD} $\times$ δ^2 and L_C = L'_{CD} $\times$ δ^2(assume the spectral index α=0), where R'_{CD} and L'_{CD} are intrinsic core dominance parameter and core luminosity respectively. Because radio galaxies are believed to be the parent population of blazars, Fan & Zhang (2003) and this work found that there is no correlation between R_{CD} and L_C for radio galaxies, which indicate that the R'_{CD} and L'_{CD} is probably not related. This suggest that the strong correlation between R_{CD} and logL_C is probably because they are both relied on δ, that means beaming play a import role in the detected radio core flux and R_{CD} is good indicator of Doppler factor, this is consistent with the beaming model of AGN (Urry & Padovani 1995). Meanwhile, for R_{CD} and L_E, there is no significant correlation; we also found there is no significant differences for the distribution of L_E between *Fermi*-QSOs and non-*Fermi*-QSOs, between Fermi-galaxie and non-Fermi galaxies, which indicate that the extend luminosity is less influenced by the beaming effect.

Because δ is important parameter for the detection of radio flux, the systematically higher mean and median radio core luminosity in FAGNs indicates that the $gamma$-ray detection of FAGNs might be caused by their higher beaming effect, while we can not exclude the possibility that their intrinsic flux might also plays a role.

3.3 The γ-ray emission and R_{CD}

We have obtained the γ-ray flux in the 100 MeV to 300 GeV energy range for 80 sources in Fan & Zhang (2003) from the 3FGL, and calculated the γ-ray luminosity. We found a strong correlation between R_{CD} and L_γ , with a correlation coefficient r=0.39 at $>$ 99.9 percent confidence level, which is shown in the left panel of Fig.5. In addition, we also consider the correlation between R_{CD} and γ-ray flux F_γ, which is shown in the right panel of Fig.5, with a correlation coefficient r=0.28 at $>$ 98 percent confidence level. Because R_{CD}= $R'_{CD}$$\times$ δ^2, these correlation might be caused by the parameters(R_{CD} L_γ and F_γ) all rely on Doppler factor δ . These results indicate that γ-ray emission is probably influenced by jet beaming effect, and R_{CD} can be treated as an indicator of the beaming effect.

4 DISCUSSION

In this work, based on a large sample of radio sources with R_{CD} (e.g., Fan & Zhang 2003), we found significant differences in R_{CD} for FAGNs and NFAGNs, *Fermi* quasars and non-*Fermi* quasars. There is a tendency that the *Fermi* sources have on average higher R_{CD} than the non-*Fermi* sources. The radio core luminosity of FAGNs are also systematically higher than NFAGNs. These results suggest that *Fermi* sources are probably with strong beaming effect, consistent with results in the literature(eg. Wu et al. (2014),Chen et al. (2015)) and indicate that R_{CD} is probably an indicator of jet beaming effect and plays an important role in the γ-ray detection among AGNs in this present sample.

4.1 The correlation between radio core flux and γ-ray emission

Ghirlanda et al. (2011), Ackermann et al. (2011) and Ackermann et al. (2015) all show that there is a statistical significant positive correlation between the centimeter radio and the γ-ray energy flux. Wu et al.

(2014) show a significant correlation between γ-ray flux and radio core flux for a sample of BL Lac objects, a similar correlation is also found for our present sample, see Fig. **??**. Because γ-ray flux and radio core flux are Doppler boosted, a strong correlation between them is expected, after excluding the common dependence on the R_{CD} which is a indicator of Doppler factor by using the partial Spearman correlation method with a correlation coefficient of 0.33 at > 99 percent level. Considering the correlation between radio core flux F_c and γ-ray flux F_γ, NFAGNs maybe have both smaller F_c and smaller F_γ, even though they have comparable R_{CD} with FAGNs. Which makes them more difficult to be detected by *Fermi*-LAT.

4.2 Why are some sources detected with *Fermi*, but others not?

Wu et al. (2014) indicate that the Doppler factor is an important parameter of γ-ray detection, the non-detection of γ-ray emission in NFBLs is likely due to low beaming effect, and/or low intrinsic γ-ray flux. The one important aim of this paper is to test if the results for BL Lac sample in Wu et al. (2014) is still valid for other type of AGN sample. We studied the differences of FAGNs and NFAGNs through radio core flux at fixed R_{CD}. In Fig.7, we show the correlation between R_{CD} and the average F_c of FAGNs and NFAGNs in R_{CD} bins similar withWu et al. (2014). The panels from left to right indicate the cases for the whole sample, quasars and galaxies, respectively (with bin size of 0.24, 0.4 and 0.28 for Log R_{CD}). From these figures, we can see that FAGNs have systematically larger radio core flux than NFAGNs at fixed R_{CD}, indicating larger intrinsic radio core flux in FAGNs, this result is in consistent with the result of BL Lac objects in Wu et al. (2014).

Because FAGNs have systematically larger radio core flux than NFAGNs at fixed R_{CD}, then their extended flux are also expected to be larger. Considering the strong linear correlation between intrinsic radio core emission and extend emission (Giovannini et al. 2001), the extended flux for FAGNs should be also larger than NFAGNs because of their systematically larger radio core flux, but no strong correlations found between extend emission and γ-ray emission for this sample. This maybe caused by our sample is small and the result indicate that the intrinsic emission are one possible factor but might not be the crucial factor for the detection of γ-ray emission as Doppler factor, further study of a larger sample of γ-ray AGNs might find the correlations between extend radio emission and γ-ray emission and test our predications.

Together with the results in Wu et al. (2014), we can see that *Fermi* detected BL Lacs, QSOs and radio galaxies all have larger intrinsic radio core flux than their non-detected samples. These results indicate a strong connection between radio and γ-ray emission for the present sample, and it seems to be in favour of the far-dissipation scenario present by Ramakrishnan et al. (2015) and Nieppola et al. (2011): a co-spatial origin of the activity for the radio and γ-ray emission, suggesting that the origin of the seed photons for the high-energy γ-ray emission is within the jet.

5 SUMMARY

In this paper, we have compared the multiple parameters for FAGNs and NFAGNs by using the available data from the literature. We found that R_{CD} have clear correlations with core luminosity, γ-ray luminosity, and γ-ray flux . The average R_{CD} in the *Fermi* sources is on average larger than that in the non-*Fermi* sources. Moreover, there is a tendency that the *Fermi* sources have higher core-luminosity than the non-*Fermi* sources for the whole sample, quasars and galaxies respectively. We also show that FAGNs have systematically larger radio core flux than NFAGNs at fixed R_{CD}, indicating larger intrinsic radio core flux in FAGNs.

Our results indicate that the R_{CD} is an important role of jet beaming effect in γ-ray detection and show that the beaming effect is vital for the detection of γ-ray emission. The non-*Fermi* sources is likely due to low beaming effect, and/or the low intrinsic γ-ray flux. The strong connections between radio and γ-ray emission might suggest that the origin of the seed photons for the high-energy γ-ray emission is within the jet for this AGN sample. On account of our sample is limited by the available archival data,

the future larger sample of new observational data including redshift, radio core luminosity, extended luminosity and γ-ray luminosity will be used for further tests of our results.

Acknowledgements We thank the anonymous referee for insightful comments and constructive suggestions. This work is supported by the National Nature Science Foundation of China (No. U1431111, 11163002, 11473054, U1531245) and by the Science and Technology Commission of Shanghai Municipality (grant 14ZR1447100)

References

Acero, F., Ackermann, M., Ajello, M., et al. 2015, ApJS, 218, 23
Ackermann, M., Ajello, M., Allafort, A., et al. 2011, ApJ, 741, 30
Ackermann, M., Ajello, M., Atwood, W. B., et al. 2015, ApJ, 810, 14
Atwood, W. B., Abdo, A. A., Ackermann, M., et al. 2009, ApJ, 697, 1071
Chen, Y. Y., Zhang, X., Zhang, H. J., & Yu, X. L. 2015, MNRAS, 451, 4193
Fan, J.-H., Yang, J.-H., Pan, J., & Hua, T.-X. 2011, Research in Astronomy and Astrophysics, 11, 1413
Fan, J. H., & Zhang, J. S. 2003, A&A, 407, 899
Fan, Z., Cao, X., & Gu, M. 2006, ApJ, 646, 8
Ghirlanda, G., Ghisellini, G., Tavecchio, F., Foschini, L., & Bonnoli, G. 2011, MNRAS, 413, 852
Giovannini, G., Cotton, W. D., Feretti, L., Lara, L., & Venturi, T. 2001, ApJ, 552, 508
Linford, J. D., Taylor, G. B., Romani, R. W., et al. 2011, ApJ, 726, 16
Linford, J. D., Taylor, G. B., Romani, R. W., et al. 2012, ApJ, 744, 177
Lister, M. L., Aller, M. F., Aller, H. D., et al. 2015, ApJL, 810, L9
Nieppola, E., Tornikoski, M., Valtaoja, E., et al. 2011, A&A, 535, A69
Orr, M. J. L., & Browne, I. W. A. 1982, MNRAS, 200, 1067
Piner, B. G., Pushkarev, A. B., Kovalev, Y. Y., et al. 2012, ApJ, 758, 84
Pushkarev, A. B., & Kovalev, Y. Y. 2012, A&A, 544, A34
Ramakrishnan, V., Hovatta, T., Nieppola, E., et al. 2015, MNRAS, 452, 1280
Urry, C. M., & Padovani, P. 1995, PASP, 107, 803
Wu, Z., Jiang, D., Gu, M., & Chen, L. 2014, A&A, 562, A64
Wu, Z., Jiang, D. R., Gu, M., & Liu, Y. 2007, A&A, 466, 63
Xiong, D., Zhang, X., Bai, J., & Zhang, H. 2015, MNRAS, 451, 2750

Table 1 The various parameters for γ-ray detected sources from Fan & Zhang (2003).

$Name$	ID	z	$logL_T$ W Hz^{-1}	$logL_C$ W Hz^{-1}	$logR_{CD}$ α_E =0.5	$logR_{CD}$ α_E =1.0	L_γ erg s^{-1}
0414+009	BL	0.287	25.30	24.70	-0.20	0.08	45.33
0521-365	BL	0.061	25.83	24.75	-0.77	-0.49	44.74
0548-322	BL	0.069	24.39	23.60	-0.44	-0.16	43.66
0723-008	BL	0.130	25.99	24.89	-0.79	-0.51	44.25
0828+493	BL	0.548	26.73	25.90	-0.48	-0.21	45.51
0829+046	BL	0.180	25.55	25.35	0.51	0.79	45.47
0954+658	BL	0.386	26.28	25.48	-0.45	-0.17	45.97
1011+496	BL	0.200	25.25	24.91	0.20	0.48	46.01
1101+384	BL	0.031	23.68	23.47	0.48	0.76	44.93
1156+295	BL	0.729	27.10	26.99	0.82	1.09	47.30
1219+285	BL	0.100	25.56	24.26	-1.00	-0.72	45.07
1413+135	BL	0.249	25.91	25.61	0.28	0.55	45.11
1652+398	BL	0.034	24.30	23.69	-0.21	0.07	44.54
1749+096	BL	0.322	26.16	25.83	0.22	0.50	46.12
1749+701	BL	0.770	27.57	26.52	-0.73	-0.46	47.10
1803+784	BL	0.680	27.34	26.97	0.15	0.42	47.08
1807+698	BL	0.050	24.84	24.60	0.41	0.68	44.36
1826+796	BL	0.664	27.39	26.88	-0.07	0.20	46.73
2131-021	BL	0.557	26.87	26.82	1.19	1.47	46.21
2200+420	BL	0.069	25.77	25.07	-0.33	-0.05	45.31
2201+044	BL	0.028	24.10	23.41	-0.31	-0.04	42.99
2240-260	BL	0.774	26.87	26.73	0.70	0.97	46.74
0305+039	G	0.029	24.83	23.77	-0.74	-0.47	43.11
0518-458	G	0.034	25.93	24.01	-1.64	-1.36	43.10
0755+379	G	0.041	24.49	23.59	-0.57	-0.29	43.05
0909+162	G	0.085	24.17	21.99	-1.90	-1.62	43.79
1010+350	G	1.414	27.14	26.87	0.34	0.62	46.91
1253-055	G	0.014	24.23	22.13	-1.82	-1.54	44.02
1322-427	G	0.001	24.62	22.12	-2.22	-1.95	41.16
1343-601	G	0.012	25.20	23.58	-1.33	-1.06	42.91
1441+522	G	0.140	25.05	23.44	-1.32	-1.05	44.06
1641+399	G	0.110	24.93	23.21	-1.44	-1.16	45.04
1823+568	G	0.088	24.84	23.65	-0.88	-0.61	44.74
1142+198	S	0.021	24.48	23.09	-1.10	-0.82	42.47
0240-002	S1	0.004	22.94	20.99	-1.67	-1.39	41.39
1637+826	S2	0.023	24.14	23.66	-0.03	0.25	43.12
0202+149	Q	0.833	27.61	27.23	0.13	0.41	46.53
0212+735	Q	2.367	28.59	28.20	0.11	0.39	47.95
0333+321	Q	1.258	28.36	27.23	-0.82	-0.54	47.26
0420-014	Q	0.915	27.82	27.26	-0.14	0.13	47.40
0528+134	Q	2.070	28.62	27.97	-0.26	0.01	48.19
0605-085	Q	0.870	27.86	27.37	-0.04	0.23	47.00
0637-752	Q	0.654	27.84	27.40	0.03	0.31	46.58
0707+476	Q	1.310	27.81	27.30	-0.07	0.20	46.96
0745+241	Q	0.410	26.56	25.88	-0.30	-0.03	45.59
0748+126	Q	0.889	27.26	27.21	1.19	1.47	46.69
0836+710	Q	2.160	28.51	27.67	-0.50	-0.22	48.10
0838+133	Q	0.684	27.23	26.45	-0.42	-0.15	46.18
0859+470	Q	1.462	28.17	27.27	-0.57	-0.29	46.83
0953+254	Q	0.712	26.66	26.53	0.73	1.01	46.44
1015+359	Q	1.226	27.18	27.16	1.60	1.88	46.57
1020+400	Q	1.254	27.51	26.70	-0.46	-0.18	46.73
1150+497	Q	0.334	26.43	25.85	-0.17	0.11	46.03
1217+023	Q	0.240	25.68	25.33	0.18	0.46	46.21
1222+216	Q	0.435	26.64	26.19	0.02	0.29	47.29
1226+023	Q	0.158	27.14	26.92	0.46	0.73	46.09
1315+346	Q	1.050	26.98	26.76	0.46	0.73	46.39
1418+546	Q	1.440	28.27	27.01	-0.96	-0.68	47.18
1451-375	Q	0.314	26.36	26.24	0.77	1.05	45.51
1508-055	Q	1.180	28.32	26.88	-1.15	-0.87	47.33
1510-089	Q	0.361	26.41	26.40	1.91	2.19	47.34
1510-089	Q	2.100	28.76	28.19	-0.16	0.12	49.21
1514-241	Q	1.546	26.64	25.49	-0.84	-0.57	47.95
1532+016	Q	1.440	27.78	27.07	-0.34	-0.06	47.06
1611+343	Q	1.401	27.88	27.78	0.86	1.14	46.99
1622-297	Q	0.815	27.26	27.18	0.97	1.25	46.96
1624+416	Q	2.550	28.57	27.99	-0.17	0.11	47.50
1633+382	Q	1.814	28.19	28.01	0.57	0.84	48.50
1638+398	Q	1.666	27.66	27.54	0.77	1.05	47.82
1800+440	Q	0.663	26.56	26.04	-0.09	0.19	46.25
1828+487	Q	0.692	27.94	27.30	-0.25	0.03	46.61
1842+681	Q	0.475	26.54	26.29	0.39	0.66	45.56
1849+670	Q	0.657	26.93	26.52	0.08	0.36	46.96
2007+777	Q	0.589	26.65	25.81	-0.50	-0.22	46.47
2037+511	Q	1.686	28.41	28.18	0.43	0.71	47.60
2145+067	Q	0.990	28.19	27.84	0.18	0.46	47.69
2201+315	Q	0.298	26.25	26.18	1.03	1.31	45.33
2230+114	Q	1.037	28.04	27.68	0.17	0.44	47.62
2251+158	Q	0.859	28.10	28.03	1.03	1.31	48.65
2335-027	Q	1.072	27.39	26.63	-0.40	-0.12	47.06

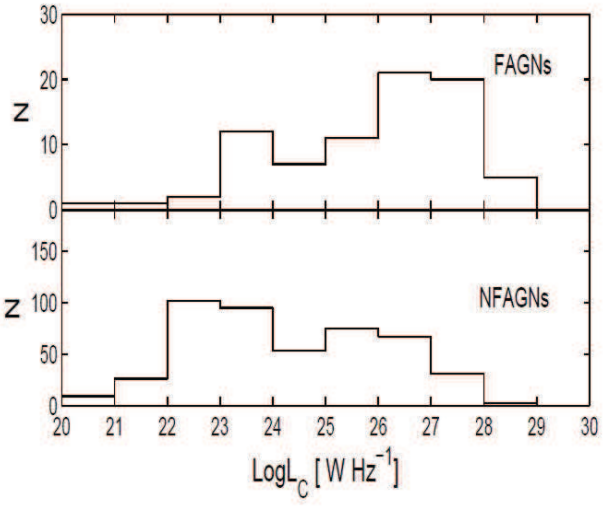

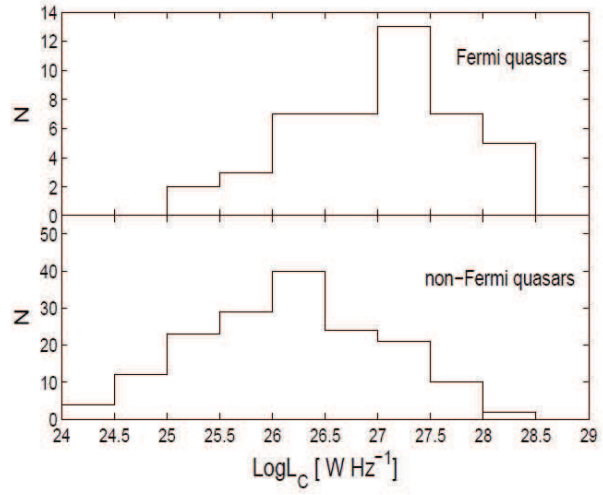

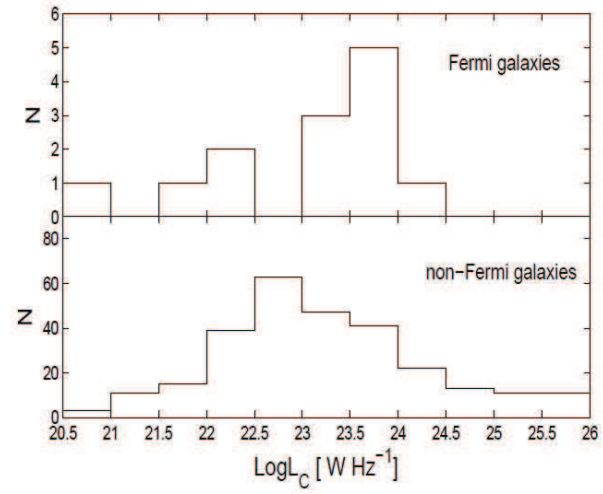

Fig. 3 The histogram comparison of core luminosity for the whole samples, quasars and galaxies.